Nonlocal nonlinear Schrödinger equation on metric graphs: A model for generation and transport of parity-time-symmetric nonlocal solitons in networks

M. Akramov,[1] K. Sabirov,[2] D. Matrasulov,[3] H. Susanto,[4] S. Usanov,[5] and O. Karpova[3]

[1]*Physics Department, National University of Uzbekistan, Vuzgorodok, Tashkent 100174, Uzbekistan*

[2]*Tashkent University of Information Technology, Amir Temur Avenue 108, Tashkent 100200, Uzbekistan*

[3]*Laboratory for Advanced Studies, Turin Polytechnic University in Tashkent, 17 Niyazov Street, 100095 Tashkent, Uzbekistan*

[4]*Department of Mathematics, Khalifa University, Abu Dhabi Campus, PO Box 127788, United Arab Emirates*

[5]*Physics Department, Yeoju Technical Institute in Tashkent, 156 Usman Nasyr Street, 100121 Tashkent, Uzbekistan*

(Received 11 January 2022; revised 13 March 2022; accepted 25 April 2022; published 16 May 2022)

We consider the parity-time (PT)-symmetric, nonlocal, nonlinear Schrödinger equation on metric graphs. Vertex boundary conditions are derived from the conservation laws. Soliton solutions are obtained for the simplest graph topologies, such as star and tree graphs. The integrability of the problem is shown by proving the existence of an infinite number of conservation laws. A model for soliton generation in such PT-symmetric optical fibers and their networks governed by the nonlocal nonlinear Schrödinger equation is proposed. Exact formulas for the number of generated solitons are derived for the cases when the problem is integrable. Numerical solutions are obtained for the case when integrability is broken.

DOI: 10.1103/PhysRevE.105.054205

I. INTRODUCTION

The parity-time (PT)-symmetric nonlocal nonlinear Schrödinger (NNLS) equation has attracted much attention since the pioneering paper by Ablowitz and Musslimani [1], where the soliton solutions are obtained using the inverse-scattering-based approach. A remarkable feature of the problem is its integrability, which was shown in [1]. Different aspects of the nonlinear nonlocal Schrödinger equation, such as integrability, various soliton solutions, and their properties have been studied over the past few years [1–13]. In [2] a discrete version of the NNLS equation was considered and its integrability was shown. In [3] an extended analysis of the NNLS equation, which includes details of the inverse scattering, Riemann-Hilbert, and Cauchy problems, was presented. In [5] exact solutions of different versions of the NNLS equation were obtained. The authos of [6] presented a study of a physically significant version of the NNLS equation, which can be derived from the Manakov system. A general soliton solution of a nonlocal nonlinear Schrödinger equation with zero and nonzero boundary conditions was derived in [9]. Quasimonochromatic complex reductions of a cubic nonlinear Klein-Gordon, the Korteweg–De Vries (KdV), and water waves equations and their relations to the nonlocal PT-symmetric nonlinear Schrödinger equation were studied in [11]. Rogue waves and periodic solutions in an NNLS-equation-based model were studied in the recent paper [13]. In this paper we consider an extension of the Ablowitz-Musslimani NNLS equation to the case of branched one-dimensional (1D) domains called the metric graphs. These are the 1D wires (bonds) connected to each other according to some rule, which is called the topology of a graph. Each bond is assumed to assigned a length. We note that the evolution equations on metric graphs are going to be a powerful tool for modeling wave propagation and particle transport in branched structures and networks (see [14–37] for a review). Using such an approach, we develop a model for the generation of PT-symmetric solitons in networks, which is described in terms of the initial value (Cauchy) problem for NNLS equation on metric graphs. THe motivation for the study of the NNLS equation on networks comes from the following facts: (i) The dynamics of solitons in networks is richer than that in line fibers; (ii) choosing the proper network architecture (topology), one can achieve the maximally acceptable soliton transport regime, i.e., tunable soliton dynamics; (iii) in many practical applications (e.g., in optoelectronics) the optical fibers appear in the form of a network, rather than as line fibers. Also, by choosing the initial pulse profile and network topology properly, one can achieve the needed number of solitons and controlled regime for soliton generation. All these make soliton dynamics in optical fiber networks more attractive than those in unbranched (line) fibers. In other words, in such structures, the branching topology can be used for the tuning of the fiber's soliton transfer properties and controlling the optical signal propagation. In particular, one can control signal loss, back scattering, and modulation by tuning the signal generation. This paper is organized as follows. In the next section we briefly recall the NNLS equation on a line, following [1]. Section III presents the formulation of the problem, its soliton solutions, and integrability for star- and tree-branched networks. In Sec. IV we provide a model for the generation of PT-symmetric nonlocal solitons in optical fiber networks. Finally, Sec. V presents some concluding remarks.

II. NONLOCAL NONLINEAR SCHRÖDINGER EQUATION ON A LINE

The PT-symmetric version of the nonlocal nonlinear Schrödinger equation on a line was proposed by Ablowitz and

Musslimani in [1] and was studied later in different contexts. Explicitly, NNLSE on a line can be written as

$$i\frac{\partial}{\partial t}q(x,t) = \frac{\partial^2}{\partial x^2}q(x,t) + 2q^2(x,t)q^*(-x,t). \tag{1}$$

Equation (1) can be rewritten as

$$\frac{\partial}{\partial t}q(x,t) = -i\frac{\partial^2}{\partial x^2}q(x,t) + iV(x,t)q(x,t), \tag{2}$$

where $V = -2q(x,t)q^*(-x,t)$ is the PT-symmetric self-induced potential. Equation (2) describes the PT-symmetric optical solitons propagating in the optical waveguide having a "gain-and-loss" structure. The one-soliton solution of Eq. (1) can be obtained using the inverse scattering method and given as [1]

$$q(x,t) = -\frac{2(\eta_1+\bar{\eta}_1)e^{i\bar{\theta}_1}e^{-4i\bar{\eta}_1^2 t}e^{-2\bar{\eta}_1 x}}{1+e^{i(\theta_1+\bar{\theta}_1)}e^{4i(\eta_1^2-\bar{\eta}_1^2)t}e^{-2(\eta_1+\bar{\eta}_1)x}}. \tag{3}$$

As it was stated in [1], solution given by Eq. (3) describes the breathing soliton, whose center of mass oscillates around a fixed point. A bright (traveling) soliton solution was found in the [7] and can be written as

$$q(x,t) = \frac{\alpha e^{\xi_1}}{1+e^{\xi_1+\bar{\xi}_1+\Delta}}, \tag{4}$$

and the parity transformed complex conjugate solution can be obtained as [7]

$$q^*(-x.t) = [q(x.t)]^*|_{x\to -x} = \frac{\beta e^{\xi_1}}{1+e^{\xi_1+\bar{\xi}_1+\Delta}}, \tag{5}$$

where $\xi_1 = ik_1x - ik_1^2t + \xi_1^{(0)}$, $\bar{\xi}_1 = i\bar{k}_1x + i\bar{k}_1^2t + \bar{\xi}_1^{(0)}$, $e^{\Delta} = -\frac{\alpha\beta}{\kappa}$, $\kappa = (k_1+\bar{k}_1)^2, k_1, \bar{k}_1, \alpha, \beta, \xi_1^{(0)}, \bar{\xi}_1^{(0)}$ are arbitrary complex constants and $\bar{k}_1, \beta, \bar{\xi}_1^{(0)}$ are complex conjugates of $k_1, \alpha, \xi_1^{(0)}$, respectively. Two conservative quantities (integrals of motion) can be determined for Eq. (1) as the norm

$$C_0(t) = \int_{-\infty}^{+\infty} q(x,t)q^*(-x,t)dx, \tag{6}$$

and the energy

$$C_2(t) = \int_{-\infty}^{+\infty}\Big[\frac{\partial}{\partial x}q(x,t)\cdot\frac{\partial}{\partial x}q^*(-x,t) + q^2(x,t)\cdot q^{*2}(-x,t)\Big]dx. \tag{7}$$

The integrability of Eq. (1) was proven in [1] by showing the existence of the infinite number of conserving quantities. In the next section we will extend the study of [1] to the case of 1D branched domains given in terms of the metric graphs.

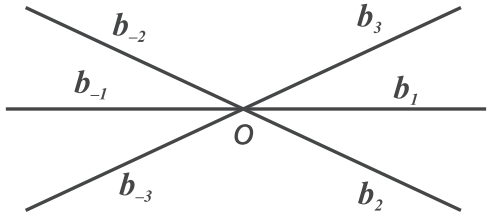

FIG. 1. Star graph with six bonds.

III. EXTENSION TO A STAR GRAPH

A. Vertex boundary conditions and soliton solutions

Consider the following nonlocal nonlinear Schrödinger equation which is written on the each bond of the star graph with six bonds $b_{\pm j}$ (see Fig. 1), for which a coordinate $x_{\pm j}$ is assigned. Choosing the origin of the coordinates at the vertex, 0 for bond b_{-j} we put $x_{-j} \in (-\infty, 0]$ and for b_j we fix $x_j \in [0, +\infty)$:

$$i\frac{\partial}{\partial t}q_{\pm j}(x,t) = \frac{\partial^2}{\partial x^2}q_{\pm j}(x,t) + \sqrt{\beta_j\beta_{-j}}q_{\pm j}^2(x,t)q_{\mp j}^*(-x,t), \tag{8}$$

where $q_{\pm j}(x,t)$ at $x \in b_{\pm j}$ and $j = 1, 2, 3$.

A very important feature of Eq. (8) is the fact that it is a system of the NNLS equations, where components of $q_{\pm j}$ are mixed in the nonlinear term. Unlike classical NLSE on graphs, where the components of the solution are related to each other via the vertex boundary conditions, in Eq. (8), components with opposite signs are mixed via the nonlinear term, while other components are connected to each other via the vertex boundary conditions. Such mixing of the components, $q_{\pm j}$ in Eq. (8) occurs due to the presence of the factor, $\sqrt{\beta_j\beta_{-j}}$. To solve Eq. (8), one needs to impose boundary conditions at the graph branching point (vertex). Such conditions can be derived from the fundamental conservation laws. Here we use the norm and the energy conservation to derive the vertex boundary conditions.

For the above nonlocal NLSE, the norm is determined as [1]

$$C_0(t) = \sum_{j=1}^{3}\Big[\int_{b_j} q_j(x,t)q_{-j}^*(-x,t)dx + \int_{b_{-j}} q_{-j}(x,t)q_j^*(-x,t)dx\Big]. \tag{9}$$

From the norm conservation, $\dot{C}_0 = 0$ we have

$$\sum_{j=1}^{3}\mathbf{Im}\Big[\frac{\partial}{\partial x}q_j(x,t)\cdot q_{-j}^*(-x,t)\Big]\Big|_{x\to+0} = \sum_{j=1}^{3}\mathbf{Im}\Big[\frac{\partial}{\partial x}q_{-j}(x,t)\cdot q_j^*(-x,t)\Big]\Big|_{x\to-0}. \tag{10}$$

Another conserving quantity, i.e., the energy is given by

$$C_2(t)=\sum_{j=1}^{3}\Bigg[\int_{b_j}\left(\frac{\partial}{\partial x}q_j(x,t)\cdot\frac{\partial}{\partial x}q^*_{-j}(-x,t)+\frac{\sqrt{\beta_j\beta_{-j}}}{2}q_j^2(x,t)\cdot q^{*2}_{-j}(-x,t)\right)dx$$
$$+\int_{b_{-j}}\left(\frac{\partial}{\partial x}q_{-j}(x,t)\cdot\frac{\partial}{\partial x}q^*_{j}(-x,t)+\frac{\sqrt{\beta_j\beta_{-j}}}{2}q_{-j}^2(x,t)\cdot q^{*2}_{j}(-x,t)\right)dx\Bigg]. \tag{11}$$

The energy conservation, $\dot{C}_2=0$ leads to

$$\sum_{j=1}^{3}\mathbf{Re}\left[\frac{\partial}{\partial t}q^*_{-j}(-x,t)\cdot\frac{\partial}{\partial x}q_j(x,t)\right]\Big|_{x\to+0}=\sum_{j=1}^{3}\mathbf{Re}\left[\frac{\partial}{\partial t}q^*_{j}(-x,t)\cdot\frac{\partial}{\partial x}q_{-j}(x,t)\right]\Big|_{x\to-0}. \tag{12}$$

Equations (10) and (12) are compatible with the following two sets of the vertex boundary conditions:

$$\alpha_1q_1(x,t)|_{x=0}=\alpha_{-1}q_{-1}(x,t)|_{x=0}=\alpha_2q_2(x,t)|_{x=0}=\alpha_{-2}q_{-2}(x,t)|_{x=0}=\alpha_3q_3(x,t)|_{x=0}=\alpha_{-3}q_{-3}(x,t)|_{x=0},$$
$$\frac{1}{\alpha_1}\frac{\partial}{\partial x}q_1(x,t)\Big|_{x=0}+\frac{1}{\alpha_2}\frac{\partial}{\partial x}q_2(x,t)\Big|_{x=0}+\frac{1}{\alpha_3}\frac{\partial}{\partial x}q_3(x,t)\Big|_{x=0}$$
$$=\frac{1}{\alpha_{-1}}\frac{\partial}{\partial x}q_{-1}(x,t)\Big|_{x=0}+\frac{1}{\alpha_{-2}}\frac{\partial}{\partial x}q_{-2}(x,t)\Big|_{x=0}+\frac{1}{\alpha_{-3}}\frac{\partial}{\partial x}q_{-3}(x,t)\Big|_{x=0}. \tag{13}$$

It should be noted that Eqs. (10) and (12) follow from the boundary conditions (13), but the opposite is not true. Let $q(x,t)$ eb the solution of the nonlocal nonlinear Schrödinger equation given by

$$i\frac{\partial}{\partial t}q(x,t)=\frac{\partial^2}{\partial x^2}q(x,t)+2q^2(x,t)q^*(-x,t). \tag{14}$$

Then the solution of the problem given by Eqs. (8) and (13) can be expressed in terms of $q(x,t)$ as $q_{\pm j}(x,t)=\sqrt{\frac{2}{\beta_{\pm j}}}q(x,t)$ and fulfills the boundary conditions (13), provided the following constraints hold true:

$$\frac{\alpha_{\pm j}}{\alpha_1}=\sqrt{\frac{\beta_{\pm j}}{\beta_1}},\quad \frac{1}{\beta_1}+\frac{1}{\beta_2}+\frac{1}{\beta_3}=\frac{1}{\beta_{-1}}+\frac{1}{\beta_{-2}}+\frac{1}{\beta_{-3}}. \tag{15}$$

One of the explicit (static) soliton solutions of Eq. (8) on a line was obtained in [3]. Using this solution, the corresponding soliton solution on a graph can be written as

$$q_{\pm j}(x,t)=-\sqrt{\frac{2}{\beta_{\pm j}}}\frac{4\eta e^{i\bar{\varphi}}e^{-4i\eta^2t}e^{-2\eta x}}{1+e^{i(\varphi+\bar{\varphi})}e^{-4\eta x}}. \tag{16}$$

φ, $\bar{\varphi}$, η are arbitrary complex constants. Similarly, one can write a traveling soliton solution as

$$q_{\pm j}(x,t)=\sqrt{\frac{2}{\beta_{\pm j}}}\frac{\alpha e^{\bar{\xi}_1}}{1+e^{\xi_1+\bar{\xi}_1+\Delta}}, \tag{17}$$

and the parity transformed complex conjugate solution

$$q^*_{\pm j}(-x,t)=\sqrt{\frac{2}{\beta_{\pm j}}}\frac{\beta e^{\xi_1}}{1+e^{\xi_1+\bar{\xi}_1+\Delta}}. \tag{18}$$

B. Integrability of the problem

Here we will show the integrability of the NNLSE on a metric star graph, given by Eqs. (8) and (13) by proving the existence of the infinite number of conservation laws. This can be done following the prescription used for the usual (not nonlocal) NLS on metric graphs in [14]. The soliton solutions of the problem on the infinite linear chain satisfy an infinite number of conservation laws given by

$$\int_{-\infty}^{+\infty}\mu_n[q(x,t),q^*(-x,t)]dx=C_n, \tag{19}$$

where C_n is a constant, μ_n is a polynomial of $q(x,t)$, $q^*(-x,t)$, and their derivatives with respect to x [3]. Using this relation, we now investigate the following quantities, which for are given on the metric star graph:

$$Q_n=\sum_{j=1}^{3}\Bigg[\beta_j^{-1}\int_{b_j}\mu_n[q(x,t),q^*(-x,t)]dx$$
$$+\beta_{-j}^{-1}\int_{b_{-j}}\mu_n[q(x,t),q^*(-x,t)]dx\Bigg], \tag{20}$$

where $q(x,t)$ is the solution of Eq. (14) and $\mu_n[q(x,t),q^*(-x,t)]$ obeys the recursion relation

$$\mu_{n+1}=q\frac{\partial}{\partial x}\left(\frac{\mu_n}{q}\right)+\sum_{m=0}^{n-1}\mu_m\mu_{n-m-1},\tag{21}$$
$$\mu_0=q(x,t)q^*(-x,t),\quad \mu_1=q(x,t)\partial_xq^*(-x,t). \tag{22}$$

Using Eq. (15), from the right-hand side (r.h.s.) of Eq. (20) we can get

$$Q_n=\left(\beta_{-1}^{-1}+\beta_{-2}^{-1}+\beta_{-3}^{-1}\right)\int_{-\infty}^{0}\mu_n[q(x,t),q^*(-x,t)]dx$$
$$+\left(\beta_1^{-1}+\beta_2^{-1}+\beta_3^{-1}\right)\int_{0}^{+\infty}\mu_n[q(x,t),q^*(-x,t)]dx$$
$$=\left(\beta_1^{-1}+\beta_2^{-1}+\beta_3^{-1}\right)\int_{-\infty}^{+\infty}\mu_n[q(x,t),q^*(-x,t)]dx$$
$$=\left(\beta_1^{-1}+\beta_2^{-1}+\beta_3^{-1}\right)C_n. \tag{23}$$

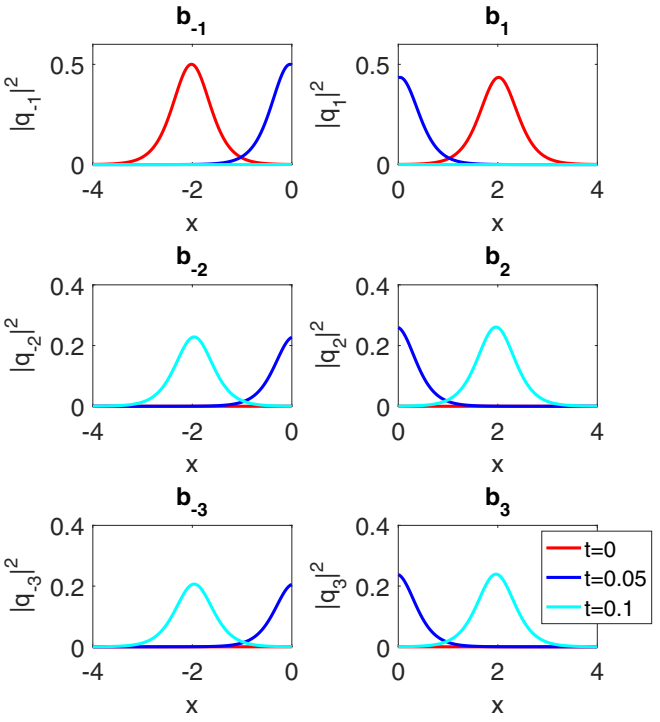

FIG. 2. Plot of soliton on a metric star graph obtained from numerical solution of Eq. (8) for the values of β_j fulfilling the sum rule in Eq. (8) ($\beta_{-1} = 1$, $\beta_1 = 1.15$, $\beta_{-2} = 2.19$, $\beta_2 = 1.91$, $\beta_{-3} = 2.42$, $\beta_3 = 2.09$). The initial conditions are given on the bonds b_{-1} and b_1.

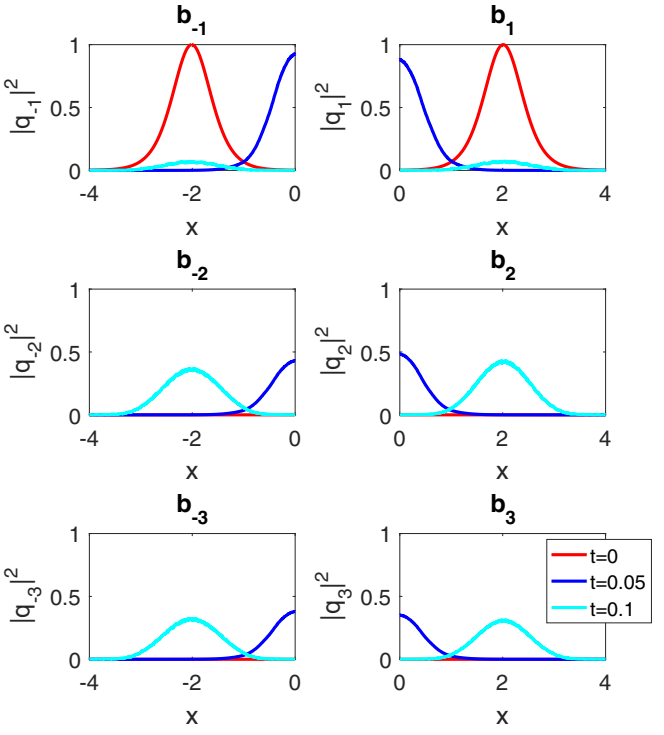

FIG. 3. Plot of soliton on a metric star graph obtained from numerical solution of Eq. (8) for the values of β_j breaking the sum rule in Eq. (8) ($\beta_{-1} = 0.65$, $\beta_1 = 0.79$, $\beta_{-2} = 2.7$, $\beta_2 = 2.09$, $\beta_{-3} = 3.06$, $\beta_3 = 2.87$). The initial conditions are given on the bonds b_{-1} and b_1.

It is clear that, due to the conservation law given by Eq. (19), Q_n is constant, i.e., conserving quantity. Therefore, Q_n is the constant of motion. This implies that the nonlocal NLSE on the metric star graph has an infinite number of conservation laws and hence is integrable.

C. Numerical results

It is clear that the above proven integrability of NNLSE (8) holds true for the case when constraints given by Eq. (15) are fulfilled. Such integrable NNLSE approves different soliton solutions, such as the breathing given by Eq. (3) and the traveling given by Eq. (4) solitons. For the case, when constraints in Eq. (15) are broken, one needs to solve Eq. (8) numerically as the initial value problem. As the initial conditions, we will choose values of exact (soliton) solutions Eqs. (17) and (18) at $t = 0$. The discretization scheme from [2] is used in the numerical solution of Eq. (1). In Fig. 2 the plots of $|q_{\pm j}(x,t)|^2$ obtained by solving Eq. (8) numerically for the initial conditions imposed on the bond b_{-1} and b_1 are presented for different time moments, $t = 0,\ \ 0.05,\ \ 0.1$ at the values of $\beta_{\pm j}$ fulfilling the sum rule in Eq. (15). A remarkable feature of the traveling solitons is the reflectionless transmission through the vertex. Figure 3 presents similar plots for those values of $\beta_{\pm j}$, which do not fulfill the sum rule in Eq. (15). Unlike the solitons in Fig. 2, the reflection at the vertex can be observed in this plot. Thus one can conclude that the integrable case provides the reflectionless transmission of solitons through the branching point of the graph. Earlier, such a feature was observed for other evolution equations on graphs, such as the NLS [14], sine-Gordon [23], and nonlinear Dirac [28] equations. The reason for such behavior of solitons described by the nonlinear Schrödinger equation on graphs was explained in [32].

D. Extension to a tree graph

The above treatment can be extended to the case's other graphs. Here we will demonstrate that for a tree graph. One of the possible tree graphs, on which one can write NNLSE, is presented in Fig. 4. The central branch, i.e., the branch at the middle of the graph, is chosen as an origin of the coordinates. Then the bonds can be determined as $b_{-1},\ b_{-1mn} \sim (-\infty; 0]$, $b_{-1m} \sim [-L_{1m}; 0]$, $b_{1m} \sim [0; L_{1m}]$, $b_1,\ b_{1mn} \sim [0; +\infty)$, where L_{1m} are the lengths of $b_{\pm 1m}$ bonds

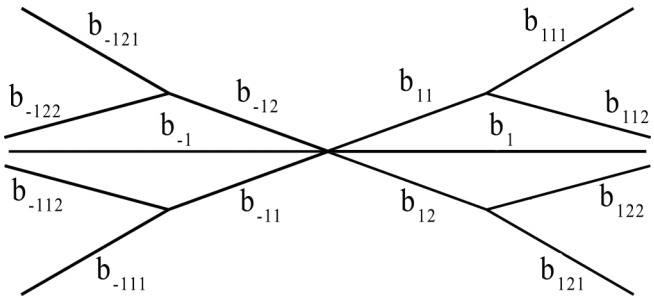

FIG. 4. A sketch of tree graph adopted for nonlocal nonlinear Schrödinger equation.

and $m = 1, 2$, $n = 1, 2$. Here the "+" sign is for right-handed bonds and the "−" sign is for left-handed bonds from the center of the tree graph.

On each bond of such a graph, one can write the nonlocal nonlinear Schrödinger equation given by Eq. (8) with $j = \pm 1,\ \pm 1m,\ \pm 1mn$.

The vertex boundary conditions following from the conservation laws are given as

$$\begin{aligned}
&\alpha_{\pm 1} q_{\pm 1}(x,t)|_{x=0} = \alpha_{\mp 11} q_{\mp 11}(x,t)|_{x=0} = \alpha_{\mp 12} q_{\mp 12}(x,t)|_{x=0},\\
&\frac{1}{\alpha_{\pm 1}} \frac{\partial}{\partial x} q_{\pm 1}(x,t)\bigg|_{x=0} = \frac{1}{\alpha_{\mp 11}} \frac{\partial}{\partial x} q_{\mp 11}(x,t)\bigg|_{x=0}\\
&\qquad + \frac{1}{\alpha_{\mp 12}} \frac{\partial}{\partial x} q_{\mp 12}(x,t)\bigg|_{x=0}, \qquad (24)\\
&\alpha_{\pm 1m} q_{\pm 1m}(x,t)|_{x=\pm L_{1m}} = \alpha_{\pm 1m1} \lim_{x\to\pm 0} q_{\pm 1m1}(x,t)\\
&\qquad = \alpha_{\pm 1m2} \lim_{x\to\pm 0} q_{\pm 1m2}(x,t),\\
&\qquad \frac{1}{\alpha_{\pm 1m}} \frac{\partial}{\partial x} q_{\pm 1m}(x,t)\bigg|_{x=\pm L_{1m}}\\
&\qquad = \frac{1}{\alpha_{\pm 1m1}} \lim_{x\to\pm 0} \frac{\partial}{\partial x} q_{\pm 1m1}(x,t)\\
&\qquad + \frac{1}{\alpha_{\pm 1m2}} \lim_{x\to\pm 0} \frac{\partial}{\partial x} q_{\pm 1m2}(x,t). \qquad (25)
\end{aligned}$$

Assuming that the following sum rules hold true:

$$\begin{aligned}
\frac{\alpha_{\pm 1}}{\sqrt{\beta_{\pm 1}}} &= \frac{\alpha_{\mp 11}}{\sqrt{\beta_{\mp 11}}} = \frac{\alpha_{\mp 12}}{\sqrt{\beta_{\mp 12}}},\\
\frac{1}{\alpha_{\pm 1}\sqrt{\beta_{\pm 1}}} &= \frac{1}{\alpha_{\mp 11}\sqrt{\beta_{\mp 11}}} + \frac{1}{\alpha_{\mp 12}\sqrt{\beta_{\mp 12}}},\\
\frac{1}{\beta_{\pm 1}} &= \frac{1}{\beta_{\mp 11}} + \frac{1}{\beta_{\mp 12}}. \qquad (26)\\
\frac{\alpha_{\pm 1m}}{\sqrt{\beta_{\pm 1m}}} &= \frac{\alpha_{\pm 1m1}}{\sqrt{\beta_{\pm 1m1}}} = \frac{\alpha_{\pm 1m2}}{\sqrt{\beta_{\pm 1m2}}},\\
\frac{1}{\alpha_{\pm 1m}\sqrt{\beta_{\pm 1m}}} &= \frac{1}{\alpha_{\pm 1m1}\sqrt{\beta_{\pm 1m1}}} + \frac{1}{\alpha_{\pm 1m2}\sqrt{\beta_{\pm 1m2}}},\\
\frac{1}{\beta_{\pm 1m}} &= \frac{1}{\beta_{\pm 1m1}} + \frac{1}{\beta_{\pm 1m2}}, \qquad (27)
\end{aligned}$$

the soliton solutions on each bond can be written as

$$\begin{aligned}
q_{\pm 1}(x,t) &= \sqrt{\frac{2}{\beta_{\pm 1}}}\, q(x + S_{\pm 1}, t),\\
q_{\pm 1m}(x,t) &= \sqrt{\frac{2}{\beta_{\pm 1m}}}\, q(x + S_{\pm 1m}, t), \qquad (28)\\
q_{\pm 1mn}(x,t) &= \sqrt{\frac{2}{\beta_{\pm 1mn}}}\, q(x + S_{\pm 1mn}, t),
\end{aligned}$$

where $S_{\pm 1} = S_{\pm 1m} = x_0$, $S_{\pm 1mn} = \pm L_{1m} + x_0$, x_0 is the coordinate of the center of the soliton at $t = 0$. The integrability of the nonlocal nonlinear Schrödinger equation on a tree graph presented in Fig. 4 (for the case when the above sum rules are fulfilled) can be shown similarly to that for the star graph. Also, one can show by numerical computations that, for the integrable case, the transmission of nonlocal PT-symmetric solitons are reflectionless. We note that the above treatment can be directly extended to other graph topologies, provided a graph consists of an even number of bonds symmetrically positioned with respect to the origin of the coordinates, i.e., one has an equal number of bonds on each side of the origin of the coordinates. In addition, at least four bonds of the graph should be semi-infinite. Unlike the solution of the usual nonlinear Schrödinger equation on graphs, the solution of the PT-symmetric nonlocal nonlinear NLSE on graphs is much more complicated which makes the dynamics of nonlocal solitons richer than that for the usual soliton. This last also implies the existence of more tools for tuning the soliton dynamics.

IV. SOLITON GENERATION

A. Soliton generation in linear PT-symmetric optical fibers

Here we consider the problem of soliton generation described in terms of the nonlocal nonlinear Schrödinger equation (1). The problem of soliton generation in optical fibers is of fundamental and practical importance for modern optoelectronics and information technologies. Hasegawa and Tappert [38] first proposed using optical solitons as carriers of information in high-speed communication systems in the early 1970s. Further development of the idea later led to advanced optoelectronic and information technologies based on the use of solitons in optical fibers (see, e.g., [39–47] for a review). The dynamics of generated solitons strongly depends on the shape of the initial pulse profile. This makes choosing an initial pulse profile an effective tool for tuning the soliton propagation. Mathematically, the problem of soliton generation is reduced to the Cauchy problem for the nonlinear evolution equation, governing the dynamics of the soliton. An important task arising in this context, besides soliton dynamics, is finding the number of generated solitons using the given initial condition. In the case of long (unbranched) fibers such a problem was studied in [48–56]. In [49], an effective method for computing the number of generated solitons was proposed. The extension of the approach for other initial pulse profiles was proposed later in [50]. The mathematical treatment of soliton generation on a half line was considered [52]. The generation in optical solitons in fibers with a dual-frequency input was considered in [53]. Soliton generation and their instability are investigated in a system of two parallel-coupled fibers, with a pumped (active) nonlinear dispersive core and a lossy (passive) linear one in [57]. Unlike the problem of soliton dynamics, studied in the previous sections, the problem of soliton generation can be reduced to an initial value problem for Eq. (1). The solution of such problems are different than those single- and multisoliton ones, obtained from inverse scattering and Hirota's method. Therefore, the shape of such generated solitons are no longer maintained during their propagation due to the radiation effects. An important task of soliton generation problem is finding the number of solitons generated for a given initial pulse profile. An effective method for solving such a task was proposed in [49], which was later applied for different types of the pulse profile in [50,53]. Thus, from the mathematical viewpoint, the problem

of generation of PT-symmetric, nonlocal solitons is given in terms of Eq. (1) for which the following initial condition is imposed:

$$q(x,0) = f(x). \tag{29}$$

The starting point in the calculation of the number of solitons generated for a given initial pulse profile is the Zakharov-Shabat problem. For Eq. (1) the Zakharov-Shabat problem is given in terms of the following AKNS system:

$$\frac{\partial v^{(1)}}{\partial x} = -ikv^{(1)} + q(x,0)v^{(2)},$$
$$\frac{\partial v^{(2)}}{\partial x} = ikv^{(2)} - q^*(-x,0)v^{(1)}. \tag{30}$$

Let us consider the special family of the initial potentials

$$q(x,0) = Q(x,0)e^{i(\delta+\pi/2)},$$
$$q^*(-x,0) = Q(-x,0)e^{-i(\delta+\pi/2)}, \tag{31}$$

where $Q(x,0)$ is the real function and $\delta\,(0 \leqslant \delta \leqslant 2\pi)$ is the arbitrary constant. One can show that the transformations

$$v^{(1)} \to V^{(1)}e^{i\gamma}, \quad v^{(2)} \to V^{(2)}e^{i(\gamma-\delta)} \tag{32}$$

lead to the following eigenvalue problem:

$$\frac{\partial V^{(1)}}{\partial x} = -ikV^{(1)} + iQ(x,0)V^{(2)},$$
$$\frac{\partial V^{(2)}}{\partial x} = ikV^{(2)} + iQ(-x,0)V^{(1)}. \tag{33}$$

Following [50], one can define the number of the zeros of the Jost coefficients $a(k)$ at $k = 0$.

If the initial condition is symmetric to the point $x = 0$: $Q(x,0) = Q(-x,0)$ then the formal solution of Eq. (33) with $k = 0$ are

$$V^{(1)}(x,0) = \exp[-iS(x)]\left(C^{(1)}\int_{-\infty}^{x} Q(x',0)\exp[2iS(x')]dx' + C^{(2)}\right),$$
$$V^{(2)}(x,0) = -iC^{(1)}\exp[iS(x)] - V^{(1)}, \tag{34}$$

where

$$S(x) = \int_{-\infty}^{x} Q(x',0)dx'.$$

If one chooses $V^{(1)}(x,0) \to 0$ for $x \to -\infty$, then $C^{(2)} = 0$, and we have

$$a(0) = \lim_{x\to+\infty} V^{(2)}(x,0)$$
$$= -iC^{(1)}\left(\exp(iS_0) - i\exp(-iS_0)\int_{-\infty}^{+\infty} Q(x,0)\exp[2iS(x))dx\right] = -iC^{(1)}\cos S_0, \tag{35}$$

where

$$S_0 = \int_{-\infty}^{+\infty} Q(x,0)dx. \tag{36}$$

From Eq. (35) for the soliton number we get

$$N = \left\langle \frac{1}{2} + \frac{S_0}{\pi} \right\rangle. \tag{37}$$

Noting that for the initial pulses given by Eq. (31) for any x and with $Q(x,0) > 0$,

$$S_0 \equiv \int_{-\infty}^{+\infty} Q(x,0)dx = \int_{-\infty}^{+\infty} |q(x,0)|dx = F, \tag{38}$$

we have, from Eqs. (37) and (38),

$$N = \left\langle \frac{1}{2} + \frac{F}{\pi} \right\rangle. \tag{39}$$

Here we consider the number of generated solitons for the rectangular initial pulse profile (see Fig. 5):

$$q(x,0) = \begin{cases} 0, & \text{for } |x| > \frac{1}{2}a, \\ b, & \text{for } |x| \leqslant \frac{1}{2}a, \end{cases} \qquad b > 0.$$

Using the above approach for this profile leads to

$$F = \int_{-\infty}^{+\infty} |q(x,0)|dx = ab, \quad N = \left\langle \frac{1}{2} + \frac{ab}{\pi} \right\rangle.$$

This equation provides the relation between the initial pulse profile and number of generated solitons, described by the PT-symmetric nonlocal nonlinear Schrödinger equation (1).

To demonstrate the soliton generation visually, in Fig. 6 we present the plots of the numerical solution of the initial value

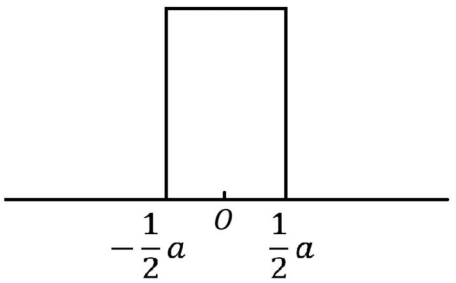

FIG. 5. Initial pulse profile.

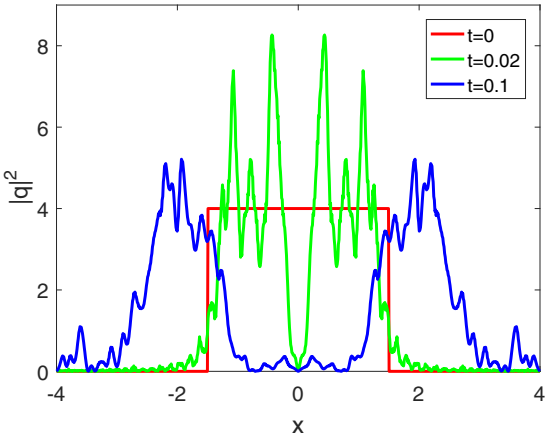

FIG. 6. Numerical solution of initial value problem given by Eqs. (1) and (29) for rectangular initial pulse profile, demonstrating generation of two solitons on a line.

problem given by Eqs. (1) and (29), where the initial pulse profile, $q(x, 0)$, is chosen in rectangular form (see Fig. 5) with $a = 3$ and $b = 2$.

B. Soliton generation in star-shaped optical waveguide network

The above approach can be applied for soliton generation in branched waveguides, by modeling these later in terms of metric graphs. Earlier, soliton generation in networks described in terms of the usual (classical) nonlinear Schrödinger equation on graphs was studied in [35]. Here we address the model for generation of PT-symmetric nonlocal solitons in a six-bond, star-branched network (see Fig. 1) described in terms of the initial value problem for Eq. (8).

Here, using the prescription of the previous section, we will provide brief derivation of the relation between the number of generated solitons and the initial pulse profile in a branched optical waveguide, which is modeled in terms of the star graph presented in Fig. 7. Consider the following Zakharov-Shabat problem for the NNLS equation (8):

$$\frac{\partial v_{\pm j}^{(1)}}{\partial x} = -ikv_{\pm j}^{(1)} + \sqrt{\frac{\beta_{\pm j}}{2}} q_{\pm j}(x,0) v_{\pm j}^{(2)},$$
$$\frac{\partial v_{\pm j}^{(2)}}{\partial x} = ikv_{\pm j}^{(2)} - \sqrt{\frac{\beta_{\mp j}}{2}} q_{\mp j}^{*}(-x,0) v_{\pm j}^{(1)}, \qquad (40)$$

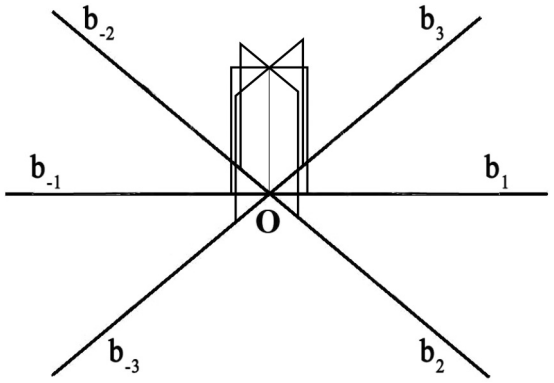

FIG. 7. Initial pulse profile for the star graph.

where $q_{\pm j}(x, 0)$ are the initial conditions (initial pulse profiles) for Eq. (8). Introducing the special family of the initial potentials given by

$$q_{\pm j}(x,0) = Q_{\pm j}(x,0) e^{i(\delta_{\pm j}+\pi/2)},$$
$$q_{\pm j}^{*}(-x,0) = Q_{\pm j}(-x,0) e^{-i(\delta_{\pm j}+\pi/2)}, \qquad (41)$$

where $Q_{\pm j}(x, 0)$ are the real functions and $\delta_{\pm j}$ ($0 \leqslant \delta_{\pm j} \leqslant 2\pi$) are arbitrary constants, one can show that the transformations

$$v_{\pm j}^{(1)} \to V_{\pm j}^{(1)} e^{i\gamma_{\pm j}}, \quad v_{\pm j}^{(2)} \to V_{\pm j}^{(2)} e^{i(\gamma_{\pm j}-\delta_{\pm j})} \qquad (42)$$

lead to the following eigenvalue problem:

$$\frac{\partial V_{\pm j}^{(1)}}{\partial x} = -ikV_{\pm j}^{(1)} + i\sqrt{\frac{\beta_{\pm j}}{2}} Q_{\pm j}(x,0) V_{\pm j}^{(2)},$$
$$\frac{\partial V_{\pm j}^{(2)}}{\partial x} = ikV_{\pm j}^{(2)} + i\sqrt{\frac{\beta_{\mp j}}{2}} Q_{\mp j}(-x,0) V_{\pm j}^{(1)}. \qquad (43)$$

From a physical viewpoint, the generation of the single quiescent soliton will occur with a smaller energy than the soliton pair. Therefore, following [50], we will define the number of the zeros of the Jost coefficients $a_{\pm j}(k)$ at $k = 0$. If the initial condition is symmetric with respect to the point $x = 0$: $Q_{\mp j}(-x, 0) = \sqrt{\frac{\beta_{\pm j}}{\beta_{\mp j}}} Q_{\pm j}(x, 0)$.

The formal solutions of Eq. (43) with $k = 0$ are

$$V_{-j}^{(1)}(x,0) = \exp[-iS_{-j}(x)]\left(C_{-j}^{(1)} \int_{-\infty}^{x} Q_{-j}(x',0) \exp[2iS_{-j}(x')]dx' + C_{-j}^{(2)}\right),$$
$$V_{-j}^{(2)}(x,0) = -iC_{-j}^{(1)} \exp[iS_{-j}(x)] - V_{-j}^{(1)},$$
$$V_{j}^{(1)}(x,0) = \exp[-iS_{j}(x)]\left(C_{j}^{(1)} \int_{0}^{x} Q_{j}(x',0) \exp[2iS_{j}(x')]dx' + C_{j}^{(2)}\right),$$
$$V_{j}^{(2)}(x,0) = -iC_{j}^{(1)} \exp[iS_{j}(x)] - V_{j}^{(1)},$$

$$S_{-j}(x) = \sqrt{\frac{\beta_{-j}}{2}} \int_{-\infty}^{x} Q_{-j}(x',0)dx',$$

and

$$S_j(x) = \sqrt{\frac{\beta_j}{2}} \int_0^x Q_j(x', 0)dx'.$$

If one chooses $V_{-j}^{(1)}(x, 0) \to 0$ for $x \to -\infty$ and $V_j^{(1)}(x, 0) \to 0$ for $x \to +0$, then $C_{\pm j}^{(2)} = 0$, and we have

$$\begin{aligned} a_{-j}(0) &= \lim_{x\to -0} V_{-j}^{(2)}(x, 0) \\ &= -iC_{-j}^{(1)}\left(\exp(iF_{-j}) - i\exp(-iF_{-j}) \int_{-\infty}^{0} Q_{-j}(x, 0)\exp[2iS_{-j}(x)]dx\right) = -iC_{-j}^{(1)}\cos F_{-j}, \end{aligned} \tag{44}$$

$$\begin{aligned} a_j(0) &= \lim_{x\to +\infty} V_j^{(2)}(x, 0) \\ &= -iC_j^{(1)}\left(\exp(iF_j) - i\exp(-iF_j) \int_{0}^{+\infty} Q_j(x, 0)\exp[2iS_j(x)]dx\right) = -iC_j^{(1)}\cos F_j. \end{aligned} \tag{45}$$

Noting that, for the initial pulses given by Eq. (41) for any x and with $Q_{\pm j}(x, 0) > 0$,

$$F_{\pm j} = \sqrt{\frac{\beta_{\pm j}}{2}} \int_{b_{\pm j}} Q_{\pm j}(x, 0)dx = \sqrt{\frac{\beta_{\pm j}}{2}} \int_{b_{\pm j}} |q_{\pm j}(x, 0)|dx. \tag{46}$$

From Eqs. (44) and (45) for the soliton number we get

$$N_{\pm j} = \left\langle \frac{1}{2} + \frac{F_{\pm j}}{\pi} \right\rangle, \quad N = \sum_{j=1}^{3}(N_{-j} + N_j). \tag{47}$$

Now consider the star graph with rectangle initial pulse (see Fig. 7). For such a profile, the initial condition is given at the vertex and can be written as $q_{\pm j}(x, 0) = \sqrt{\frac{2}{\beta_{\pm j}}}\psi_{\pm j}(x)$:

$$\psi_{-j}(x) = \begin{cases} 0, & \text{for } x < -\frac{1}{2}a, \\ b, & \text{for } -\frac{1}{2}a \leqslant x \leqslant 0, \end{cases}$$

$$\psi_j(x) = \begin{cases} 0, & \text{for } x > \frac{1}{2}a, \\ b, & \text{for } 0 \leqslant x \leqslant \frac{1}{2}a, \end{cases}$$

where $b > 0$.

The number of generated solitons can be written as

$$F_{\pm j} = \sqrt{\frac{\beta_{\pm j}}{2}} \int_{b_{\pm j}} |q_{\pm j}(x, 0)|dx = \frac{ab}{2},$$

$$N = 6\left\langle \frac{1}{2} + \frac{ab}{2\pi} \right\rangle. \tag{48}$$

Another initial pulse profile is the Gaussian one, given by

$$q_{\pm j}(x, 0) = \sqrt{\frac{2}{\beta_{\pm j}}} A \exp\left[-\frac{1}{2}(1 - i\alpha)\left(\frac{x}{\sigma}\right)^{2m}\right]. \tag{49}$$

Utilizing the above approach for this profile leads to

$$F_{\pm j} = \sqrt{\frac{\beta_{\pm j}}{2}} \int_{b_{\pm j}} |q_{\pm j}(x, 0)|dx = \frac{2^{\frac{1}{2m}} A\sigma}{2m}\Gamma\left(\frac{1}{2m}\right),$$

$$N = 6\left\langle \frac{1}{2} + \frac{2^{\frac{1}{2m}} A\sigma}{2\pi m}\Gamma\left(\frac{1}{2m}\right) \right\rangle.$$

We note that Eq. (47) for the number of generated solitons is derived under the assumption that the sum rule in Eq. (15) is fulfilled, which is equivalent to the integrability of the NNLS equation on the graph. For the case, when the sum rule is broken, one needs to solve the problem numerically, by imposing, e.g., the initial conditions given by Eq. (49). The plots of the soliton profiles obtained by numerical solution of Eq. (8) are presented in Fig. 8 for the time moments, $t = 0$, $t = 0.06$, and $t = 0.12$. The same discretization scheme as in the previous section is used for the numerical solution of the initial value problem for the NNLS equation on a star graph. An important feature of the soliton generation, i.e., breaking of the initial pulse profile due to the radiation can be observed from the plots of Fig. 8.

Again, to show the soliton generation visually, in Fig. 9, presents the plots of the numerical solution of the initial value

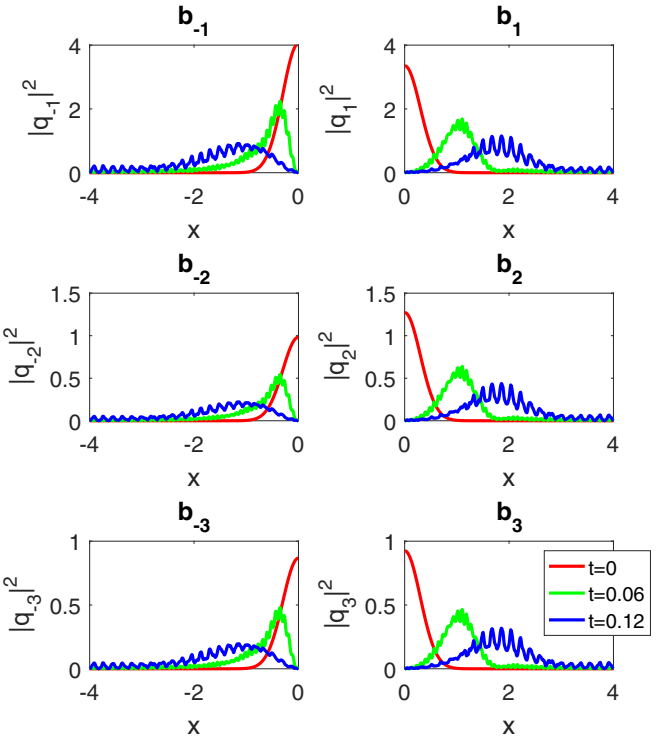

FIG. 8. Evolution of the solitons profile on time at $t = 0$ (red line), $t = 0.06$ (green line), and $t = 0.12$ (blue line) on the star graph, showing the radiation during the soliton propagation.

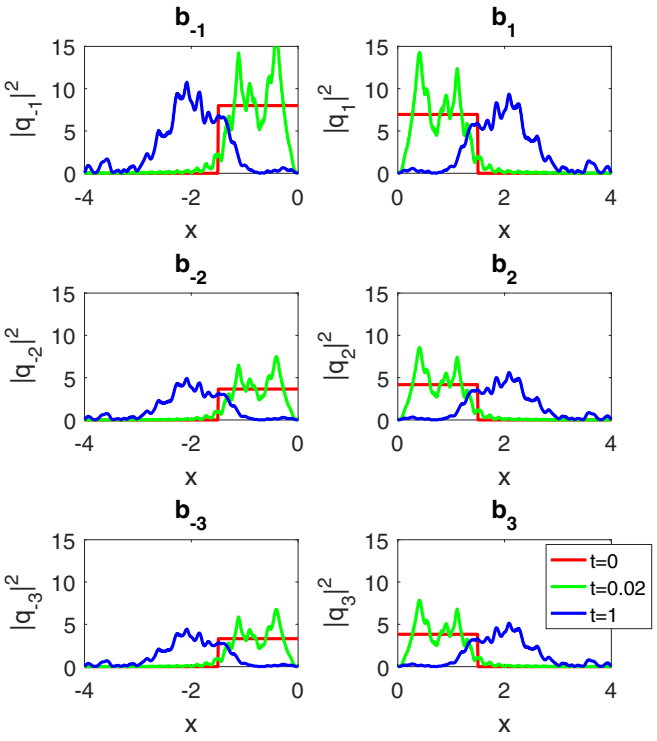

FIG. 9. Numerical solution of initial value problem given by Eqs. (8) and (13), for the initial rectangular pulse profile (see Fig. 7), demonstrating generation of six solitons on a star graph. The nonlinearity coefficients are chosen as $\beta_{-1} = 1$, $\beta_1 = 1.15$, $\beta_{-2} = 2.19$, $\beta_2 = 1.91$, $\beta_{-3} = 2.42$, $\beta_3 = 2.09$.

problem given by Eqs. (8) and (13), by imposing the initial condition in the form of the rectangular pulse (see Fig. 7) with $a = 3$ and $b = 2$. The sizes of the initial pulses, i.e., the values of a and b correspond to the generation of six solitons in Eq. (48).

C. Extension to a tree graph

The approach developed in the previous subsection can be extended for modeling of soliton generation in arbitrary networks. Here we demonstrate this for tree-branched networks presented in Fig. 4. Choosing the initial pulse profile at each vertex $[q_e(x,0) = \sqrt{\frac{2}{\beta_e}}\psi_e(x)]$ in the forms (see Fig. 10)

$$\psi_{\pm 1}(x) = \begin{cases} 0, & |x| > \frac{1}{2}a, \\ A, & 0 \leqslant |x| \leqslant \frac{1}{2}a, \end{cases}$$

$$\psi_{\pm 1m}(x) = \begin{cases} A, & 0 \leqslant |x| \leqslant \frac{1}{2}a, \\ 0, & \frac{1}{2}a < |x| < L_{1m} - \frac{1}{2}a, \\ A_n, & L_{1m} - \frac{1}{2}a \leqslant |x| \leqslant L_{1m}, \end{cases}$$

$$\psi_{\pm 1mn}(x) = \begin{cases} A_n, & 0 \leqslant |x| \leqslant \frac{1}{2}a, \\ 0, & |x| > \frac{1}{2}a, \end{cases}$$

for the number of solitons we have

$$N_e = \left\langle \frac{1}{2} + \frac{F_e}{\pi} \right\rangle, \quad N = \sum_{e \in \Omega} N_e, \tag{50}$$

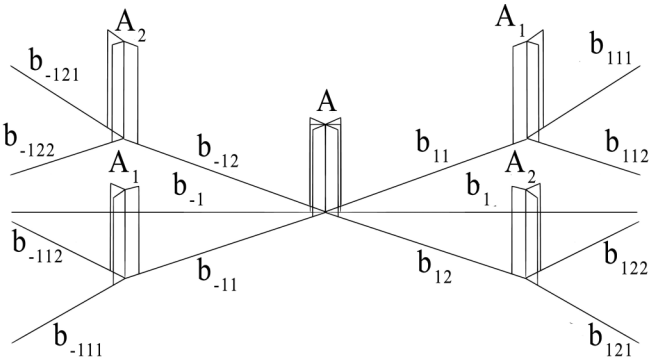

FIG. 10. Initial pulse profile for the tree graph.

where $\Omega = \{\pm 1; \pm 1m; \pm 1mn\}$ and

$$F_{\pm 1} = \sqrt{\frac{\beta_{\pm 1}}{2}} \int_{b_{\pm 1}} |q_{\pm 1}(x,0)| dx = \frac{aA}{2},$$

$$F_{\pm 1m} = \sqrt{\frac{\beta_{\pm 1m}}{2}} \int_{b_{\pm 1m}} |q_{\pm 1m}(x,0)| dx = \frac{a}{2}(A + A_m),$$

$$F_{\pm 1mn} = \sqrt{\frac{\beta_{\pm 1mn}}{2}} \int_{b_{\pm 1mn}} |q_{\pm 1mn}(x,0)| dx = \frac{aA_m}{2}.$$

Again, for the case, when the constraints given by Eqs. (26) and (27) are not fulfilled, Eq. (50) cannot be used for finding the number of solitons generated and the NNLS equation should be solved numerically.

V. CONCLUSION

In this paper we studied the dynamics of solitons described by PT-symmetric nonlocal nonlinear Schrödinger equation on networks by modeling these later in terms of metric graphs. The integrability of the problem in the case of fulfilling certain constraints given in terms of nonlinearity coefficients is shown. Exact soliton solutions, which are valid for this case, are obtained. For the case, when the constraints are broken the problem is solved numerically. The analysis of the soliton dynamics shows the absence of the back scattering in the transmission of the soliton through the graph node, is the sum rule in Eq. (15) is fulfilled. When this sum rule is broken, the transmission is accompanied by the scattering of solitons at the node. The treatment is extended for the tree graph and the possibility for the extension for other complicated graphs is discussed. The problem of generation of PT-symmetric nonlocal solitons is also studied with the focus on the calculation of the (generated) soliton number. A model for the generation of (more than one) solitons from a given initial pulse in line and branched optical fibers is proposed. The exact expression for the number of solitons generated is derived. In the case of optical waveguide networks, the problem is solved for star- and tree-branched networks. The approach used in this paper can be directly extended to arbitrary network topologies. The above model can be applied for describing the soliton generation and propagation in optical fiber networks, where each branch has self-induced gain-loss and other branched waveguides generating a self-induced PT-symmetric potential. The experimental realization of such

a model is of importance for the engineering and practical implementation of PT-symmetric optical fiber networks, capable of generating solitonic pulses and tunable signal propagation.

[1] M. J. Ablowitz and Z. H. Musslimani, Phys. Rev. Lett. **110**, 064105 (2013).
[2] M. J. Ablowitz and Z. H. Musslimani, Phys. Rev. E **90**, 032912 (2014).
[3] M. J. Ablowitz and Z. H. Musslimani, Nonlinearity **29**, 915 (2016).
[4] M. J. Ablowitz and Z. H. Musslimani, Stud. Appl. Math. **139**, 7 (2017).
[5] D. Sinha and P. K. Ghosh, Phys. Rev. E **91**, 042908 (2015).
[6] J. Yang, Phys. Rev. E **98**, 042202 (2018).
[7] S. Stalin, M. Senthilvelan, and M. Lakshmanan, Phys. Lett. A **381**, 2380 (2017).
[8] Z. Wen and Zh. Yan, Chaos **27**, 053105 (2017).
[9] B.-F. Feng, X.-D. Luo, M. J. Ablowitz, and Z. H. Musslimani, Nonlinearity **31**, 5385 (2018).
[10] M. J. Ablowitz, X.-D. Luo, and Z. H. Musslimani, J. Math. Phys. **59**, 011501 (2018).
[11] M. J. Ablowitz and Z. H. Musslimani, J. Phys. A: Math. Theor. **52**, 15LT02 (2019).
[12] J. Rao, J. He, T. Kanna, and D. Mihalache, Phys. Rev. E **102**, 032201 (2020).
[13] C. B. Ward, P. G. Kevrekidis, T. P. Horikis, and D. J. Frantzeskakis, Phys. Rev. Research **2**, 013351 (2020).
[14] Z. Sobirov, D. Matrasulov, K. Sabirov, S. Sawada, and K. Nakamura, Phys. Rev. E **81**, 066602 (2010).
[15] K. Nakamura, Z. A. Sobirov, D. U. Matrasulov, and S. Sawada, Phys. Rev. E **84**, 026609 (2011).
[16] R. Adami, C. Cacciapuoti, D. Finco, and D. Noja, Rev. Math. Phys. **23**, 409 (2011).
[17] K. K. Sabirov, Z. A. Sobirov, D. Babajanov, and D. U. Matrasulov, Phys. Lett. A **377**, 860 (2013).
[18] D. Noja, Philos. Trans. R. Soc. A **372**, 20130002 (2014).
[19] H. Uecker, D. Grieser, Z. Sobirov, D. Babajanov, and D. Matrasulov, Phys. Rev. E **91**, 023209 (2015).
[20] D. Noja, D. Pelinovsky, and G. Shaikhova, Nonlinearity **28**, 2343 (2015).
[21] R. Adami, C. Cacciapuoti, and D. Noja, J. Diff. Eq. **260**, 7397 (2016).
[22] V. Caudrelier, Commun. Math. Phys. **338**, 893 (2015).
[23] Z. Sobirov, D. Babajanov, D. Matrasulov, K. Nakamura, and H. Uecker, Europhys. Lett. **115**, 50002 (2016).
[24] R. Adami, E. Serra, and P. Tilli, Commun. Math. Phys. **352**, 387 (2017).
[25] A. Kairzhan and D. E. Pelinovsky, J. Phys. A: Math. Theor. **51**, 095203 (2018).
[26] K. K. Sabirov, S. Rakhmanov, D. Matrasulov, and H. Susanto, Phys. Lett. A **382**, 1092 (2018).
[27] K. K. Sabirov, J. Yusupov, D. Jumanazarov, and D. Matrasulov, Phys. Lett. A **382**, 2856 (2018).
[28] K. K. Sabirov, D. B. Babajanov, D. U. Matrasulov, and P. G. Kevrekidis, J. Phys. A: Math. Theor. **51**, 435203 (2018).
[29] D. Babajanov, H. Matyoqubov, and D. Matrasulov, J. Chem. Phys. **149**, 164908 (2018).
[30] D. U. Matrasulov, J. R. Yusupov, and K. K. Sabirov, J. Phys. A: Math. Theor. **52**, 155302 (2019).
[31] J. R. Yusupov, K. K. Sabirov, M. Ehrhardt, and D. U. Matrasulov, Phys. Lett. A **383**, 2382 (2019).
[32] J. R. Yusupov, K. K. Sabirov, M. Ehrhardt, and D. U. Matrasulov, Phys. Rev. E **100**, 032204 (2019).
[33] J. R. Yusupov, Kh. Sh. Matyokubov, K. K. Sabirov, and D. U. Matrasulov, Chem. Phys. **537**, 110861 (2020).
[34] D. Matrasulov, K. Sabirov, D. Babajanov, and H. Susanto, Europhys. Lett. **130**, 67002 (2020).
[35] K. K. Sabirov, M. E. Akramov, R. Sh. Otajonov, and D. U. Matrasulov, Chaos, Solitons Fractals **133**, 109636 (2020).
[36] K. K. Sabirov, J. R. Yusupov, M. M. Aripov, M. Ehrhardt, and D. U. Matrasulov, Phys. Rev. E **103**, 043305 (2021).
[37] K. K. Sabirov, J. R. Yusupov, M. Ehrhardt, and D. U. Matrasulov, Phys. Lett. A **423**, 127822 (2022).
[38] A. Hasegawa and F. Tappert, Appl. Phys. Lett. **23**, 142 (1973).
[39] L. F. Mollenauer, R. H. Stolen, and J. P. Gordon, Phys. Rev. Lett. **45**, 1095 (1980).
[40] V. E. Zakharov and A. B. Shabat, Sov. Phys. JETP **34**, 62 (1972).
[41] *Solitons*, edited by R. K. Bullough and P. J. Caudrey (Springer, Berlin, 1980).
[42] A. C. Scott, F. Y. F. Chu, and D. W. McLaughlin, Proc. IEEE **61**, 1443 (1973).
[43] J. Satsuma and N. Yajima, Prog. Theor. Phys. Suppl. **55**, 284 (1974).
[44] A. Hasegawa and Y. Kodama, Proc. IEEE **69**, 1145 (1981).
[45] *Optical Solitons: Theory and Experiment*, edited by J. R. Taylor (Cambridge University Press, Cambridge, England, 1992).
[46] A. Hasegawa and Y. Kodama, *Solitons in Optical Communications* (Oxford University Press, Oxford, 1995).
[47] Y. Kivshar and G. Agrawal, *Optical Solitons: From Fibers to Photonic Crystals* (Elsevier Science, Amsterdam, 2003).
[48] T. Dauxois and M. Peyrard, *Physics of Solitons* (Cambridge University Press, Cambridge, England, 2006).
[49] J. Burzlaff, J. Phys. A: Math. Gen. **21**, 561 (1988).
[50] Y. S. Kivshar, J. Phys. A: Math. Gen. **22**, 337 (1989).
[51] S. A. Gredeskul and Y. S. Kivshar, Phys. Rev. Lett. **62**, 977 (1989).
[52] A. S. Fokas and A. R. Its, Phys. Rev. Lett. **68**, 3117 (1992).
[53] N.-C. Panoiu, I. V. Mel'nikov, D. Mihalache, C. Etrich, and F. Lederer, Phys. Rev. E **60**, 4868 (1999).
[54] N. Nishizawa, R. Okamura, and T. Goto, Jpn. J. Appl. Phys. **38**, 4768 (1999).
[55] D. V. Skryabin and A. V. Yulin, Phys. Rev. E **72**, 016619 (2005).
[56] X. Zhong, N. Yao, J. Sheng, and K. Cheng, Opt. Laser Technol. **99**, 1 (2018).
[57] R. Ganapathy, B. A. Malomed, and K. Porsezian, Phys. Lett. A **354**, 366 (2006).